SPECTRAL, OPTICAL, AND BIREFRINGENCE STUDIES OF ZnO DISPERSED SCHIFF BASED LIQUID CRYSTALS COMPOUNDS FOR DISPLAY DEVICE APPLICATION**

P. Jayaprada [1], R. K. N. R. Manepalli [2*], B. T. P. Madhav [3], P. Pardhasaradhi [3], M. C. Rao [1]

[1] Department of Physics, Andhra Loyola College, Vijayawada, India
[2] Department of Physics, Andhra University, Vishakhapatnam, India; e-mail: manepalli.67@gmail.com
[3] LCRC-R&D, Department of ECE, Koneru Lakshmaiah Education Foundation, Guntur, India

Nowadays zinc nanoparticles (NPs) have attracted many applications in display technology. Due to the dispersion of nanoparticles in liquid crystals (LCs), the display properties are enhanced. The present work focuses on the significant changes in the properties of LC displays with the dispersion of ZnO NPs. Schiff-based LC compounds like p-n-decyloxybenzaldehyde and corresponding p-n-alkoxyanilines (10O.Om, with m = 3, 6) are prepared with the dispersion of ZnO NPs (1 wt%). The tools used to characterize the nanoparticles in LCs are X-ray diffraction (XRD), scanning electron microscopy (SEM), differential scanning calorimetry (DSC), polarizing optical microscopy (POM), and modified spectrometer. With XRD studies, the size of ZnO NPs is determined. By using SEM and EDS, the homogeneous dispersion and elemental analysis is estimated. With the data of POM, the textural analysis is examined. With DSC, the phase transition temperature of different phases is noted. With the modified spectrometer, the values of refractive indices and birefringence are determined. Furthermore, with these values, the molecular orientational order parameter S is measured by the Kuczynski and Haller Extrapolation methods. It is observed that the birefringence and order parameter values are decreased with the dispersion of 1 wt% ZnO NPs in Schiff based LC compounds.

Keywords: *synthesis, nanodispersion, X-ray diffraction, polarizing optical microscopy, differential scanning calorimetry, dispersive power.*

СПЕКТРАЛЬНЫЕ, ОПТИЧЕСКИЕ СВОЙСТВА И ДВУЛУЧЕПРЕЛОМЛЕНИЕ ЖИДКОКРИСТАЛЛИЧЕСКИХ СОЕДИНЕНИЙ НА ОСНОВЕ ШИФФА С ДИСПЕРСНЫМИ НАНОЧАСТИЦАМИ ZnO ДЛЯ ПРИМЕНЕНИЯ В УСТРОЙСТВАХ ОТОБРАЖЕНИЯ

P. Jayaprada [1], R. K. N. R. Manepalli [2*], B. T. P. Madhav [3], P. Pardhasaradhi [3], M. C. Rao [1]

УДК 532.783;620.3

[1] Колледж Андхра Лойола, Виджаявада, Индия
[2] Университет Андхра, Вишакхапатнам, Индия; e-mail: manepalli.67@gmail.com
[3] Образовательный фонд Конеру Лакшмайя, Гунтур, Индия

(Поступила 10 июня 2022)

Описаны существенные изменения свойств жидкокристаллических (ЖК) дисплеев при дисперсии наночастиц (НЧ) ZnO. ЖК-соединения на основе Шиффа — п-н-децилоксибензальдегид и соответствующие п-н-алкоксианилины (10O.Om, m = 3, 6) — получены с дисперсией НЧ ZnO (1 мас.%). Для характеристики НЧ в ЖК использованы рентгеновская дифракция, сканирующая электронная микроскопия (СЭМ), дифференциальная сканирующая калориметрия (ДСК), поляризационная оптическая микроскопия (ПОМ) и модифицированный спектрометр. На основе рентгеноструктурных исследований определен размер НЧ ZnO, с помощью СЭМ оценена однородность дисперсии, на основе ЭДС и ПОМ осуществлены элементный и текстурный анализ. Температура фазового перехода

** Full text is published in JAS V. 90, No. 4 (http://springer.com/journal/10812) and in electronic version of ZhPS V. 90, No. 4 (http://www.elibrary.ru/title_about.asp?id=7318; sales@elibrary.ru).

установлена методом ДСК. С помощью модифицированного спектрометра определены показатели преломления и двулучепреломления. Параметр молекулярного ориентационного порядка измерен методами экстраполяции Кучинского и Галлера. Обнаружено, что двулучепреломление и параметр порядка уменьшаются при диспергировании 1 мас.% НЧ ZnO в ЖК-соединения на основе Шиффа.

Ключевые слова: *синтез, нанодисперсия, рентгеноструктурный анализ, поляризационная оптическая микроскопия, дифференциальная сканирующая калориметрия, дисперсионная способность.*

Introduction. Organic materials are very attractive and have fascinating flow properties like fluids and order properties like crystals known as liquid crystals (LCs). These materials have mobility and order for the synthesis and self-assembly of liquid crystal molecules at the nanoscale level [1, 2]. These materials are very important because they exhibit very high electro-optic and thermo-optic effects due to high birefringence [3] and large dielectric anisotropy [4]. The inclusion of nanoparticles (NPs) in LC matrices induces great changes obtained at the nanoscale level such as LC alignment, electro-optical properties [5–9], and stabilization of phases of LCs [10, 11]. The nanoparticles of zinc oxide have special features like large exciton binding energy, high optical bandgap, UV random lasing amplified photoluminescence and a large quantum confinement effect [12–17]. Dispersion of ZnO NPs in LC materials can influence the long-range orientational order and also affect optical properties like electrical and electro-optical transition temperatures of phases and textures of LCDs. Dispersion of ZnO NPs in liquid crystals also affects the low threshold voltage, decreasing the relaxation frequency and memory effects [18–20]. ZnO NPs dispersed LCs results in reducing the undesired field screening effect [21]. The LC molecules oriented around a particular direction are called orientational order parameters in nematic LCs. The smectic LCs exhibited two ways of orientational and positional order. Both order parameters Σ and *S* are important because they reveal the properties of LCs and their applications in various fields. These are temperature dependent and from the experimental data, it is evident that order parameters play a critical role in LC displays of nematic and smectic phases.

The present paper primarily focuses on the optical properties of dispersion of 1 wt% ZnO NPs in respective LC compounds *p*-*n*-decyloxybenzaldehyde and the corresponding *p*-*n*-alkoxyanilines (10O.O*m*). 10O.O*m* means *p*-*n*-decyloxybenzaldehyde corresponding *p*-*n*-alkoxy anilines where *m* = 3, 6. The chemical structure is represented in the following. The name of the compounds in the short notation is 10O.O*m* (10O.O3 and 10O.O6). DSC and POM are used to determine the phase changes of pure and LC nanocomposites of *p*-*n*-decyloxybenzaldehyde and corresponding *p*-*n*-alkoxyanilines with respect to temperature. The morphological information and elemental analysis of 1 wt% dispersed ZnO NPs in 10O.O*m* LC compounds can be obtained with SEM and EDS. The refractive indices (RI) are measured by the modified spectrometer with high accuracy using different wavelengths of 460, 500, 570, and 635 nm. From data of RI, it is observed that birefringence as well as order parameter values are decreased with the dispersion of 1 wt% ZnO NPs in Schiff-based LC compounds.

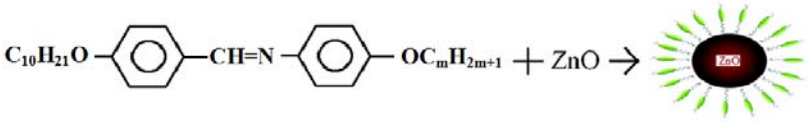

m = 3 *p*-*n*-decyloxybenzaldehyde and *p*-*n*-propoloxy anilines
m = 6 *p*-*n*-decyloxybenzaldehyde and *p*-*n*-hexyloxy anilines

Experimental. For the current work, the LC compounds, *p*-*n*-decyloxybenzaldehyde and *p*-*n*-alkoxy anilines (10O.O*m*, *m* = 3, 6) were purchased from Sigma Aldrich Laboratories, USA and used as such. The corresponding LC compounds were dissolved in ethyl alcohol and stirred for 45 m and later 1 wt% ZnO NPs were introduced into the mesongenic material of LC compounds in the isotropic state [22].

The grain sizes of ZnO NPs that are dispersed in 10O.O*m* LC compounds are determined by XRD. SEM and EDS (Zeiss special addition – 18 make) are used to determine size, shape, and chemical analysis. Instruments like the polarizing microscope (POM-SDTECHS make SDVPM2727) and the differential scanning calorimeter (DSC-Perkin Elmer Diamond) were used to find transition temperatures, phases of LCs such as nematic and smectic, enthalpy values of pure 10O.O*m* (*m* = 3, 6) and 1 wt% dispersed ZnO NPs. A modified spectrometer (SDTECHS make 6336) indigenously designed and fabricated was used to calculate refractive indices and the birefringence of 10O.O*m* pure and LC ZnO nanocomposites.

Results and discussion. The XRD pattern of pure and 1 wt% dispersed ZnO NPs in 10O.O*m* LC compounds are shown in Fig. 1. The raw data of 10O.O3 with 1 wt% ZnO NPs match with the JCPDS card No. 00-005-0011 and the raw data of 10O.O6 with 1 wt% ZnO match with the JCPDS card number 00-048-2146. The size can be calculated using formula $t = k\lambda/(\beta\cos\theta)$ and the size of ZnO NPs is 70 nm; β is FWHM. The peaks observed at angles 20.35, 23.51, 29.18, 22.90, 40.54, and 50.59° represent the confirmation of ZnO nanoparticles dispersed in LC compounds of 10O.O*m*. SEM and EDS are used to study the homogeneous dispersion and elemental analysis of pure 10O.O*m* and 1 wt% dispersed ZnO NPs. From this technique, the topological information and the presence of ZnO NPs in atomic weight percentages is known. SEM images and EDS data of pure LC and 10O.O6 LC ZnO nanocomposites are presented in Fig. 2. The information obtained from SEM image gives the presence of ZnO NPs in 10O.O6 LC compound.

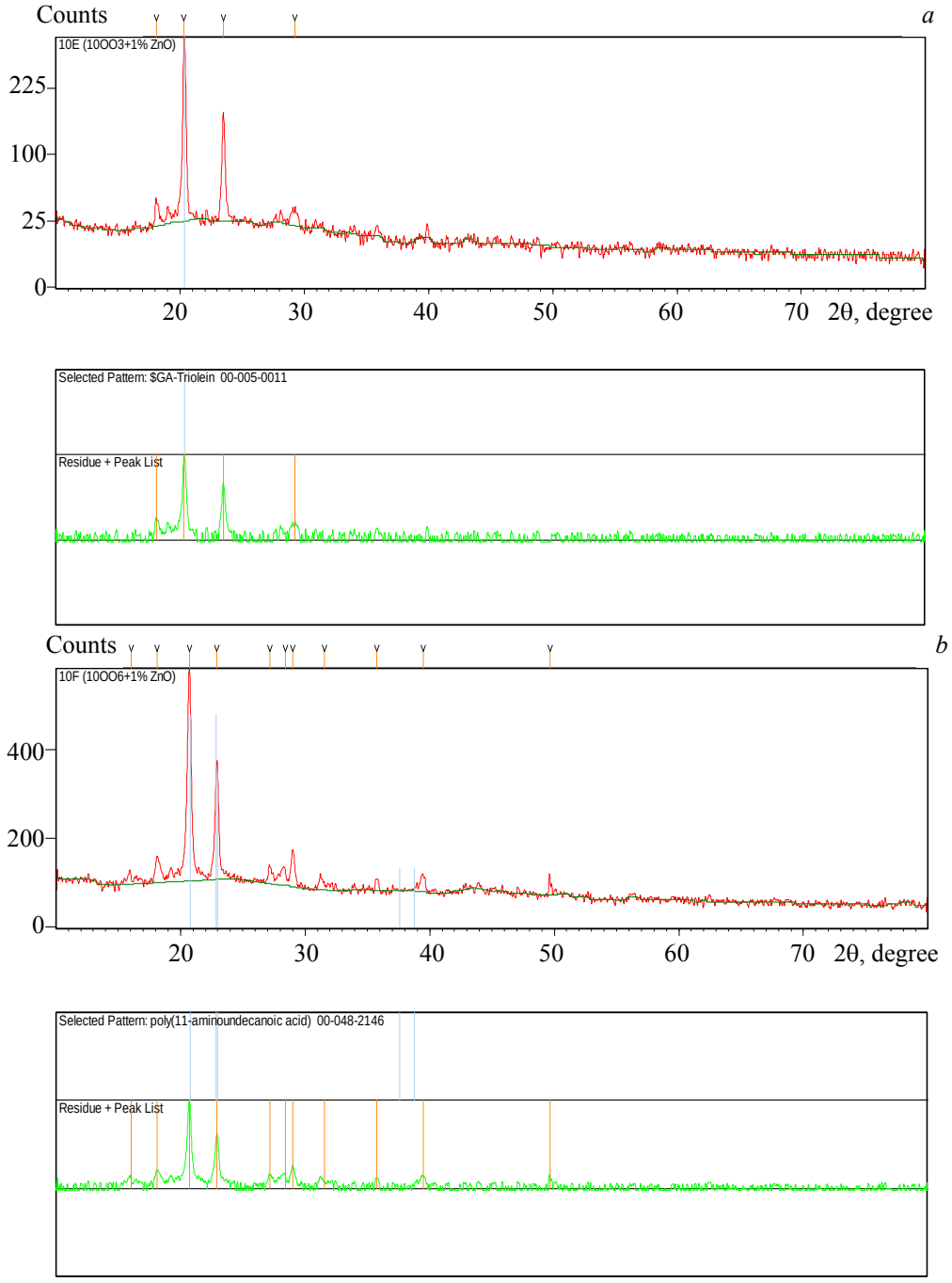

Fig. 1. XRD pattern of (a) 10O.O3 pure with 1 wt% ZnO NPs, (b) 10O.O6 pure with 1 wt% ZnO NPs.

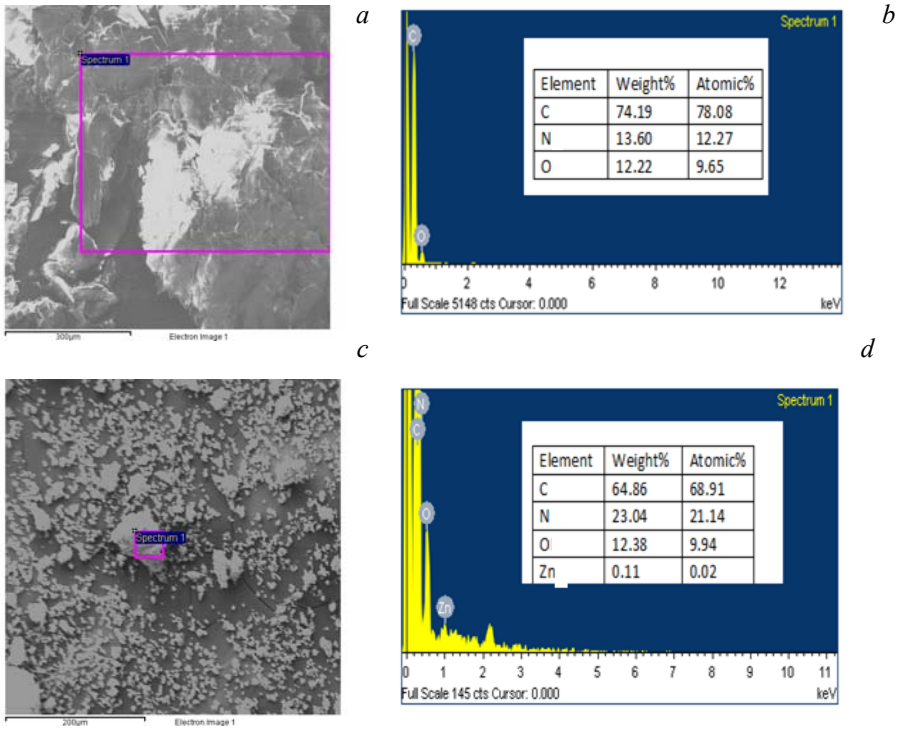

Fig. 2. SEM image of pure 10O.O6 (a) and 10O.O6 + 1 wt% ZnO NPs(c), EDS data of pure 10O.O6 (b) and 10O.O6 + 1 wt% ZnO NPs (d).

From the optical polarizing microscopy, the transition temperatures of different phases of pure 10O.O6 LC compound and 1 wt% dispersed ZnO NPs are presented in Fig. 3. POM contains a heating block, which is always maintained at a temperature accuracy of ±0.1°C with a magnification of 10X. The temperature variation of the heating block is maintained with voltage variac. 10O.O6 LC nanocomposite is placed on the heating block arranged with a glass plate having a cover slip. The textures are studied with CCD camera connected to POM, which reduces the temperature in the isotropic state.

The peaks obtained with differential scanning calorimetry (DSC) with the dispersion of 1 wt% ZnO NPs in 10O.O6 LC compound are presented in Fig. 4 for both cooling and heating. The transition temperature obtained with DSC and the phases obtained at different transition temperatures with POM are nearly in agreement and both are complementary to each other. The variation of temperatures for both tools is very small. The pure and 10O.O6 LC compounds exhibit different phases of smectics such as smectic-A, smectic-C, and smectic-G. With the dispersion of 1 wt% ZnO NPs, the same phases are obtained but nematic temperature

TABLE 1. Transition Temperatures of DSC and POM of 10O.O*m* compounds

Compound	DSC/ POM	Transition temperature, °C						Nematic range	Smectic ranges
		I-N	N-A	A-C	C-I/C-B	I-G	G-K/B-K		
10O.O3	DSC	105.00	98.18	86.26			81.73	6.82	11.92
	POM	104.9	97.90	86.40	88.40		83.30	7.00	11.5
10O.O3+1% ZnO NPs	DSC ΔH, J/g	104.31 –3.4126	97.40 2.5862	85.95 1.6363	83.39 29.8900		78.20 22.48	6.91	
	POM	103.20	95.60	84.70	82.80		77.90	7.6	11.45
10O.O6	DSC	111.07			91.65		75.02		
	POM	110.20	105.80	94.0	88.80	83.8	73.9	4.4	5.2
10O.O6+1% ZnO NPs	DSC ΔH, J/g	109.62 11.031			89.58 3.5144		72.01 49.8703		
	POM	110.50	104.40	93.1	91.70	77.8	73.80	6.1	1.4

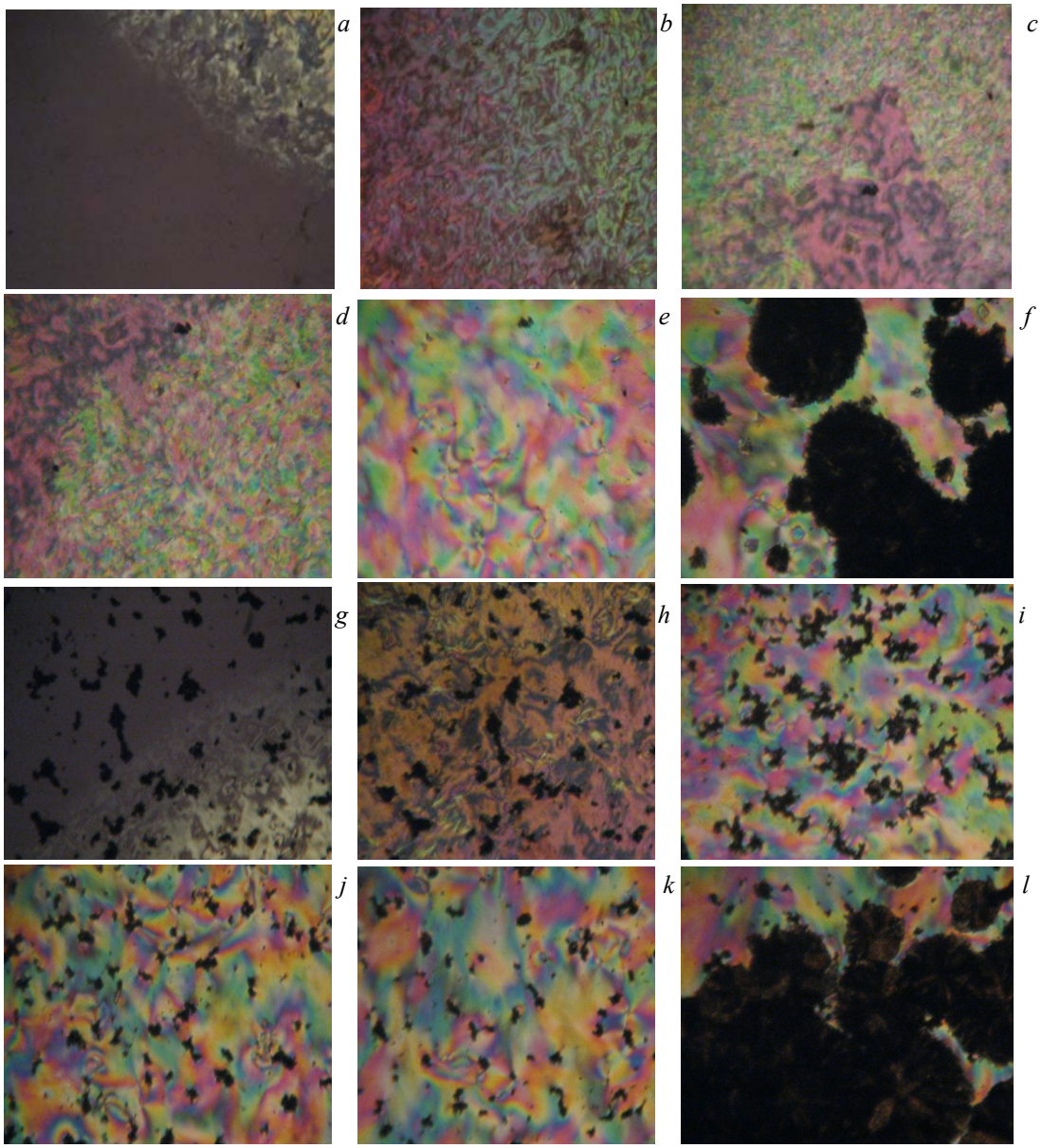

Fig. 3. POM image of pure 10O.O6 (a) nematic at 110.20ºC, (b) smectic-A at 105.8ºC, (c) smectic-C at 93.1ºC, (d) smectic-I at 91.7ºC, (e) smectic-G at 77.8ºC, (f) solid at 73.8ºC, POM image of 10O.O6 + 1 wt% ZnO NPs (g) nematic at 110.50ºC, (h) smectic-A at 104.4ºC, (i) smectic-C at 94.0ºC, (j) smectic-I at 88.0ºC, (k) smectic-G at 83.8ºC, (l) solid at 77.9ºC.

ranges are increased and smectic ranges are quenched. The transition temperatures obtained with both tools are presented in Table 1.

With the modified spectrometer, the refractive indices of pure 10O.O*m* and LC ZnO nanocomposites are calculated and presented in Fig. 5. From the data of n_e and n_o, the birefringence values are also calculated; that is the difference between the extraordinary ray and ordinary ray ($n_e - n_o$) which is denoted by δn.

At a particular region, the variation between n_e and n_o is very small and almost constant within the small temperature range and it is called FDNLR region. In this region, the nematic phase is stabilized. It is very useful for display devices. The birefringence of 10O.O3 and 10O.O6 ZnO nanocomposites calculated at various wavelengths (460, 500, 570, and 635 nm) with decreasing temperatures are shown in Fig. 6. The values of birefringence are decreased while adding 1 wt% ZnO NPs in 10O.O*m* LC compounds in comparison with nematic thermal ranges of pure 10O.O*m* and 10O.O*m* LC ZnO nanocomposites. The smectic phase ranges are more than the nematic thermal ranges.

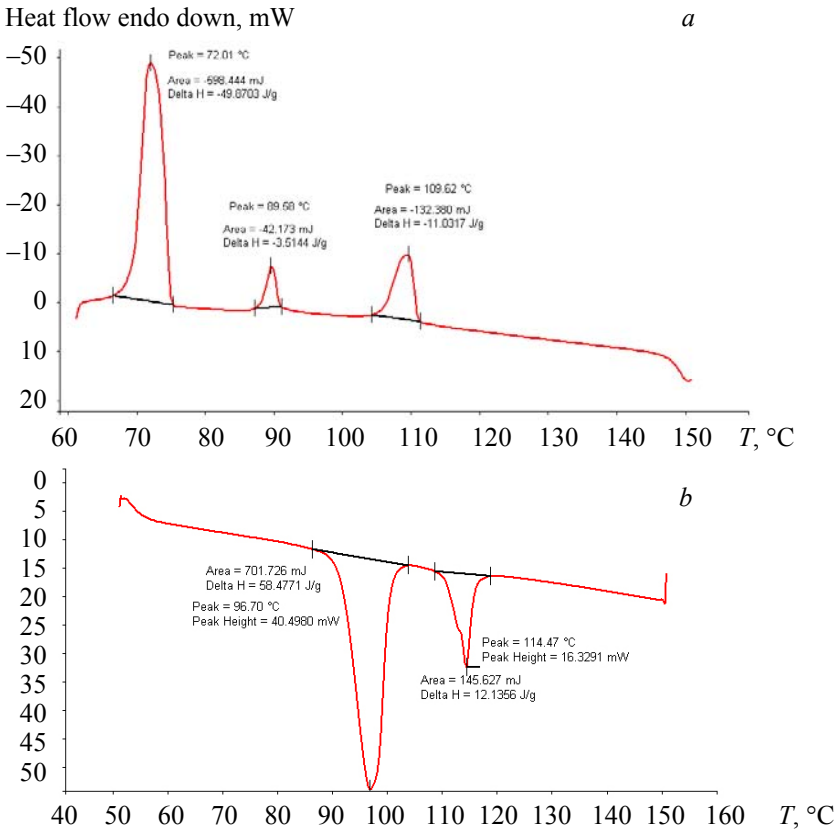

Fig. 4. DSC thermograms of 10O.O6 with 1 wt% ZnO NPs (a) cooling, (b) heating.

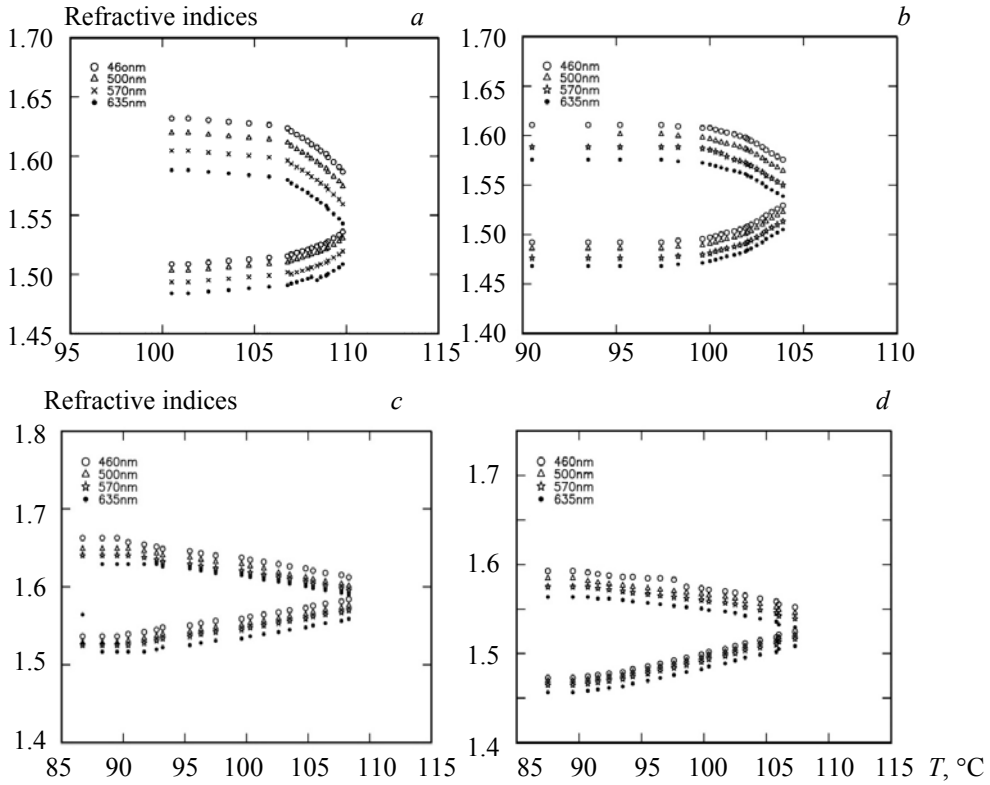

Fig. 5. Temperature vs n_e and n_o at various wavelengths 460, 500, 570, and 635 nm: (a) 10O.O3 pure, (b) 10O.O3 with 1 wt% ZnO NPs, (c) 10O.O6 pure, (d) 10O.O6 pure with 1 wt% ZnO NPs.

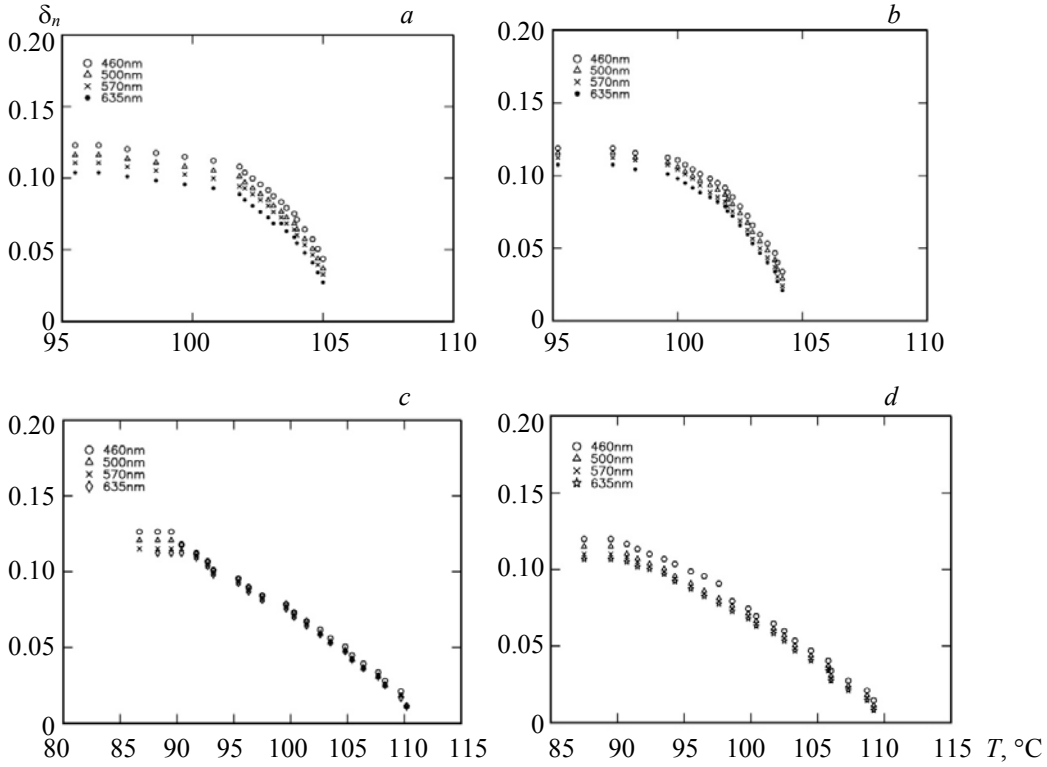

Fig. 6. Temperature dependence of birefringence (δ*n*) at various wavelengths 460, 500, 570, and 635 nm: (a) 10O.O3 pure, (b) 10O.O3 with 1 wt% ZnO NPs, (c) 10O.O6 pure, and (d) 10O.O6 pure with 1 wt% ZnO NPs.

The tendency to rotate the molecules of LC compound towards the direction of a director is called order parameter *S*. The order parameter can be explained by physical properties such as birefringence and viscosity of the nematic LC compounds. The order parameter is calculated in liquid crystals for display properties. Nematic LCs have a very long-range orientational order, which is helpful to align the liquid crystalline molecules with more order. From Kuczynski, the orientational order parameter of the molecules of pure LC compounds and with the dispersion of ZnO NPs is estimated by the following equation,

$$S = \delta n/\Delta n, \tag{1}$$

where *S* is the orientational order parameter, $\delta n = n_e - n_o$ is the difference between the refractive indices of the extraordinary ray and ordinary ray, and Δn is the birefringence anisotropy in perfect order.

Haller [23] has given a new approach to calculate the order parameter while ignoring the influence of internal molecular fields in the LC materials:

$$S_{\text{Haller}} = [1 - T/T_{\text{NI}}]^{\beta}, \tag{2}$$

where T_{NI} is known as clearing temperature or I-N transition temperature, and slope β is obtained from Kuczynski method.

From the values of n_e and n_o, the order parameter can be estimated with various methods like the Kuczynski and Haller extrapolation methods [24]. It is found that the order parameter is decreased with the dispersion of 1 wt% ZnO NPs in 10O.O*m* LC compounds [25, 26]. The order parameters of pure 10O.O*m* LC and 1 wt% dispersed ZnO NPs of 10O.O*m* measured from the Kuczynski and Haller extrapolation methods are presented in Figs. 7 and 8. The order parameter values obtained (Kuczynski and Haller extrapolation method) from Eqs. (1) and (2) are presented in Table 2. It is clear that 10O.O*m* LC compounds exhibit both orientational and transitional order. On dispersion of 1 wt% ZnO NPs in 10O.O*m* LC compounds, the order parameter values are decreased. Though the alkyl chain length of 10O.O*m* compounds is very large and nematic phase exhibits only orientational order, the smectic phase exhibits both orientational and transitional order. In 10O.O*m* LC compounds, the nematic range is enhanced for pure LC compounds, and with the dispersion of 1 wt% ZnO NPs in 10O.O*m* LCs, the smectic range is quenched. Thus, the nematic range is wider

in 10O.O*m* LCs than in the smectic range. Although the nematic range is increased in 10O.O*m* LC compounds with a dispersion of 1 wt% ZnO NPs, the orientational order is decreased. Due to the localized defects, the reorientation takes place between LC and NPs and makes the reorientation of LCs harder and it is the cause of the disorder [27].

The values of refractive indices of ordinary and extraordinary rays are calculated with the modified spectrometer at various wavelengths 460, 500, 570, and 635 nm in the visible region of the stabilized nematic phase [28]. It consists of a wedge-shaped cell with a small angled prism that houses the material called the dispersive power of the material for this particular color, which indicates the ability of the LC material in the wedge-shaped cell to disperse the light rays. The dispersive powers are calculated from the values of refractive indices of extraordinary and ordinary rays. The value of dispersive powers can be calculated for the different colors of the LC material. The value of ω can be calculated with the equation

$$\omega = (\delta_b - \delta_r)/\delta. \quad (3)$$

The dispersive powers of pure 10O.O6 and 10O.O3 LC compounds and also with 1 wt% dispersed ZnO NPs determined for various wavelengths (460, 500, 570, and 635 nm) are presented in Table 3.

TABLE 2. Order Parameter (*S*) Values from Kuczynski and Haller Extrapolation Method

Compound	Kuczynski method				Haller extrapolation method			
	460 nm	500 nm	570 nm	635 nm	460 nm	500 nm	570 nm	635 nm
10O.O3 pure	0.4380	0.4282	0.4181	0.4130	0.6299	0.6157	0.6177	0.6059
10O.O3 +1 wt% ZnO NPs	0.4284	0.4213	0.4096	0.4054	0.5915	0.5769	0.5707	0.5526
10O.O6 pure	0.7540	0.7454	0.7320	0.7306	0.7183	0.7147	0.7022	0.6987
10O.O6 +1 wt% ZnO NPs	0.7048	0.6879	0.6717	0.6560	0.6975	0.6819	0.6722	0.6709

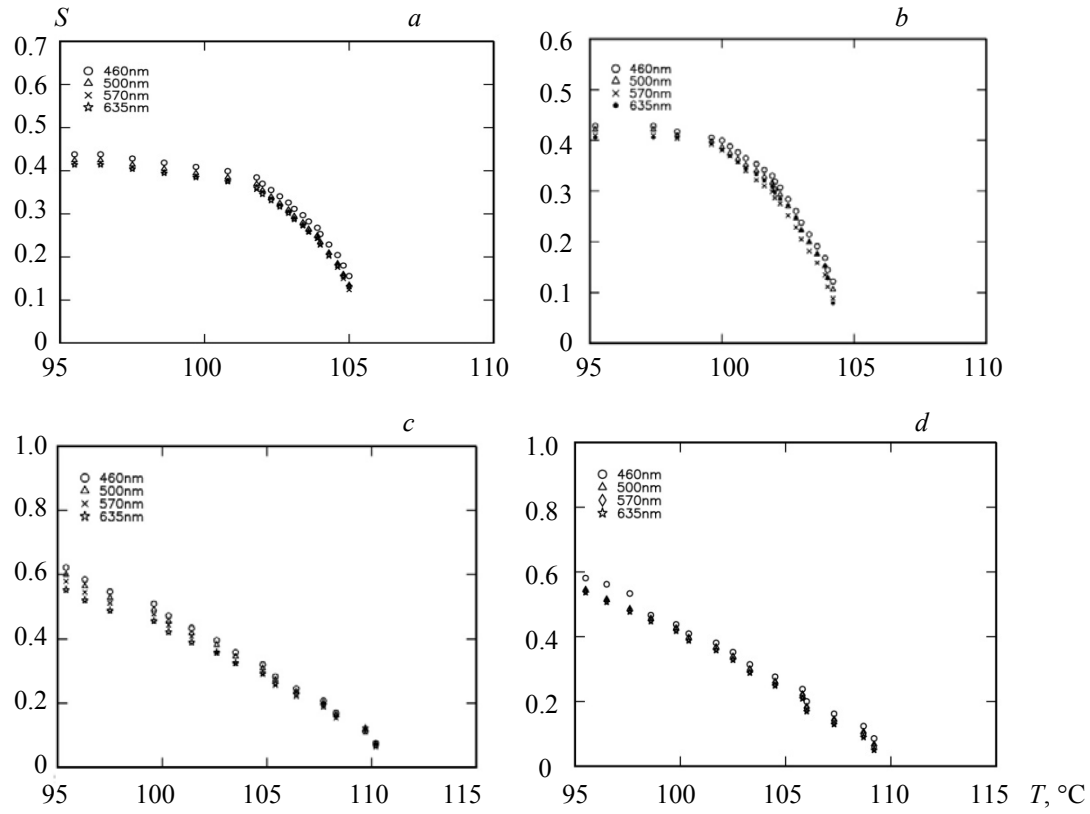

Fig. 7. Variation of *S* with temperature at various wavelengths 460, 500, 570, and 635 nm: (a) 10O.O3 pure, (b) 10O.O3 with 1 wt% ZnO NPs, (c) 10O.O6 pure, (d) 10O.O6 with 1 wt% ZnO NPs *via* the Kuczynski method.

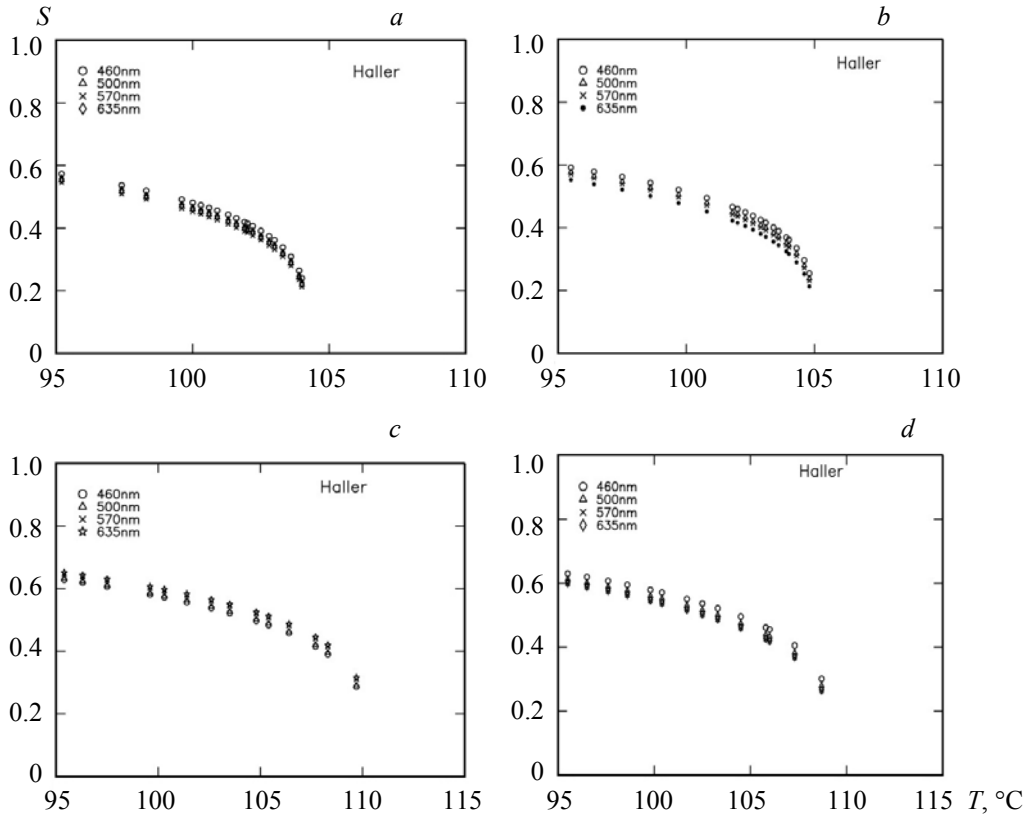

Fig. 8. Variation of *S* with temperature at various wavelengths 460, 500, 570, and 635 nm: (a) 10O.O3 pure, (b) 10O.O3 with 1 wt% ZnO NPs, (c) 10O.O6 pure, (d) 10O.O6 with 1 wt% ZnO NPs *via* the Haller extrapolation method.

TABLE 3. Dispersive Powers (ω) of 10O.O3 and 10O.O6 Pure LC Compounds with Dispersion of 1 wt% ZnO Nanoparticles

RI	Red-yellow	Red-green	Red-blue	Yellow-green	Yellow-blue	Green-blue
10O.O3 pure						
ω	0.0227	0.0441	0.0587	0.0213	0.0357	0.0143
ω_e	0.0275	0.0520	0.0532	0.0245	0.0442	0.0196
ω_o	0. 0271	0. 0396	0.0500	0.0192	0.0331	0.0138
10O.O3 +1 wt% ZnO NPs						
ω	0.0190	0.0396	0.0532	0.0205	0.0348	0.0142
ω_e	0.0220	0.0435	0.0500	0.0215	0.0136	0.0158
ω_o	0.0195	0.0387	0. 0495	0.0008	0.0300	0.0108
10O.O6 pure						
ω	0.0167	0.0252	0.0432	0.0130	0.0265	0.0180
ω_e	0.0200	0.0430	0.0521	0.0132	0.0344	0.0214
ω_o	0.0261	0.0533	0.0373	0.0533	0.0211	0.0158
10O.O6 + 1 wt% ZnO NPs						
ω	0.0185	0.0314	0.0411	0.0129	0.0221	0.0096
ω_e	0.0199	0.0366	0.0235	0.0167	0.0305	0.0137
ω_o	0.0175	0.0279	0.0348	0.0103	0.0171	0.0068

The deviations for red and blue color are represented by δ_b and δ_r, δ is the mean deviation such that,

$$\delta_b = (n_b - 1)\alpha, \quad (4)$$

$$\delta_r = (n_r - 1)\alpha, \quad (5)$$

$$\delta = (n - 1)\alpha. \quad (6)$$

The mean refractive index for the color blue is represented by n_b for LC/LC nanocomposites, for the color red the mean refractive index is denoted by n_r, the mean refractive index

$$n = (n_b + n_r)/2. \quad (7)$$

The wedge-shaped angle is represented by α. It is very small and the dispersive power of the material can be calculated with the formulae

$$\omega = (n_b - n_r)/(n - 1), \quad (8)$$

$$\omega = dn/(n - 1). \quad (9)$$

Dispersive power is mainly used in geometrical optics and stated in terms of refractive indices for red and blue and mean refractive index. It is also observed that the dispersive power is independent of the angle of the prism and the angle of the incidence. The dispersive powers of 10O.O*m* LC compounds are decreased with the dispersion of 1 wt% ZnO NPs.

The LC compounds almost attain the constant value of birefringence in the infrared region at which the vibrational bands of LC molecules are at resonance [29]. LC compounds exhibit the property of birefringence and it is decreased with respect to wavelength in the visible region; however, it remains the same in the IR region. Cauchy has derived a formula using the values of refractive indices of n_e and n_o which can be fitted to two approximations for dispersion in far absorption [30]. Cauchy derived a three-coefficient model temperature dependent on liquid crystals for the determination of refractive indices. The three-band method is more fit to the values of refractive indices of liquid crystals than the two-coefficient model. Three-coefficient model is used for high birefringence LCs and a two-coefficient model is used for low birefringent LCs. The major absorption of a LC compound occurs in two spectral regions: ultraviolet (UV) and infrared (IR). $\sigma\rightarrow\sigma^*$ electronic transitions take place in the vacuum UV (100–180 nm) region, whereas $\pi\rightarrow\pi^*$ electronic transitions occur in the UV (180–400 nm) region. If a LC compound has a longer conjugation, its electronic transition wavelength would extend to a longer UV wavelength. In the near IR region, some overtone molecular vibration bands appear. The three-band model was derived based on the LC absorption spectra by taking three main electronic transitions into consideration: one $\sigma\rightarrow\sigma^*$ transition (λ_0-band) and two $\pi\rightarrow\pi^*$ transitions (λ_1- and λ_2-bands).

The refractive index of the three-band model is represented by the following expressions,

$$n_e \cong 1 + g_{0e}\frac{\lambda^2\lambda_0^2}{\lambda^2 - \lambda_0^2} + g_{1e}\frac{\lambda^2\lambda_1^2}{\lambda^2 - \lambda_1^2} + g_{2e}\frac{\lambda^2\lambda_2^2}{\lambda^2 - \lambda_2^2}, \quad (10)$$

$$n_o \cong 1 + g_{0o}\frac{\lambda^2\lambda_0^2}{\lambda^2 - \lambda_0^2} + g_{1o}\frac{\lambda^2\lambda_1^2}{\lambda^2 - \lambda_1^2} + g_{2o}\frac{\lambda^2\lambda_2^2}{\lambda^2 - \lambda_2^2}, \quad (11)$$

where λ_0, λ_1, and λ_2 (with $\lambda_2 > \lambda_1$) denote the resonance wavelengths of one $\sigma\rightarrow\sigma^*$ and two $\pi\rightarrow\pi^*$ transitions and g_0, g_1, and g_2 are the corresponding proportionality constants that depend on the oscillator strength and temperature. For a conjugated LC molecule, its λ_0 band is located in the vacuum UV region ($\lambda_0 \sim 120$ nm), λ_1 is around 190–210 nm and not too sensitive to the LC structure, and λ_2 increases substantially as the molecular conjugation increases. In the present study, for LC compounds (*p*-*n*-decyloxybenzaldehyde and *p*-*n*-alkoxy anilines (10O.O*m*, *m* = 3, 6)), $\lambda_1 \sim 210$ nm and $\lambda_2 \sim 285$ nm.

The value of the RI (refractive index) of the material can be derived from Cauchy's equation for any wavelength and is determined by the following formula

$$n(\lambda) = A + B/\lambda^2. \quad (12)$$

The values of *A* and *B* are denoted as Cauchy's constants for a particular material for a known wavelength, λ is the wavelength, and *n* is the refractive index. Three-band model describes the origins of refractive indices of LC compounds. However, a commercial mixture usually consists of several compounds with different molecular structures in order to obtain a wide nematic range. The individual λ_i's are, therefore, different so that Eq. (10) would have too many unknowns to describe the refractive indices of a LC mixture. To model the refractive indices of a LC mixture, we could expand Eq. (10) into power series because in visible and IR spectral regions $\lambda > \lambda_2$. By keeping up to λ^{-4} terms, we derive the extended Cauchy model.

The anisotropic nature of the material is determined by the equation [31]

$$n_e(\lambda) = A_e + B_e/\lambda^2 + C_e/\lambda^4. \quad (13)$$

The values of Cauchy's coefficients A_e, B_e, and C_e for the extraordinary ray are

$$A_e = 1 + g_{0e}\lambda_0^2 + g_{1e}\lambda_1^2 + g_{2e}\lambda_2^2, \quad (14)$$

$$B_e = g_{0e}\lambda_0^4 + g_{1e}\lambda_1^4 + g_{2e}\lambda_2^4, \quad (15)$$

$$C_e = g_{0e}\lambda_0^6 + g_{1e}\lambda_1^6 + g_{2e}\lambda_2^6, \quad (16)$$

$$n_o(\lambda) = A_o + B_o/\lambda^2 + C_o/\lambda^4. \quad (17)$$

The values of Cauchy's coefficients A_o, B_o, and C_o for the ordinary ray are

$$A_o = 1 + g_{0o}\lambda_0^2 + g_{1o}\lambda_1^2 + g_{2o}\lambda_2^2, \quad (18)$$

$$B_o = g_{0o}\lambda_0^4 + g_{1o}\lambda_1^4 + g_{2o}\lambda_2^4, \quad (19)$$

$$C_o = g_{0o}\lambda_0^6 + g_{1o}\lambda_1^6 + g_{2o}\lambda_2^6, \quad (20)$$

$$n_e(\lambda) = A_e + B_e/\lambda^2, \quad (21)$$

$$n_o(\lambda) = A_o + B_o/\lambda^2. \quad (22)$$

Several authors have attempted to fit the refractive indices of anisotropic liquid crystals using Cauchy's equations [32]. Cauchy's equation provides an empirical way of describing the relationship of various refractive indices of liquid crystal with the wavelength of light. It is often difficult to measure individual refractive indices (n_e and n_o) at several wavelengths and birefringence ($\Delta n = n_e - n_o$). Cauchy's equation describes the dependence of two refractive indices n_e and n_o and Δn as a function of wavelength. The values of birefringence for the pure compound of 10O.O3 at various wavelengths are 0.12305 (460 nm), 0.1162 (500 nm), 0.11077 (570 nm), and 0.1039 (635 nm), whereas for the dispersed 1 wt% ZnO compound, the values of birefringence are 0.1186 (460 nm), 0.1154 (500 nm), 0.1125 (570 nm) and 0.1074 (635 nm). For the compound of 10O.O6, the values of birefringence are 0.1198 (460 nm) 0.1157 (500 nm), 0.1142 (570 nm) and 0.1068 (635 nm), whereas for dispersed 1 wt% ZnO NPs, the values are 0.1157 (460 nm), 0.1142 (500 nm), 0.1125 (570 nm) and 0.1054 (635 nm). The three-coefficient Cauchy model fits high birefringence LCs ($\Delta n > 0.2$) more accurately than the two-coefficient model. For low birefringence LC mixtures ($\Delta n < 0.12$), the two-coefficient Cauchy model works equally as well as the three-coefficient model in the off-resonance spectral region. Based on the values of birefringence from the data of refractive indices of 10O.Om (m = 3,6) for LCs and their nanocomposites, the two-coefficient Cauchy model is more fit to find the parameters than the three-coefficient Cauchy model (three-band model). The single-band model [29, 33] gives an explicit expression of the wavelength and temperature dependence for birefringence, but not for the individual refractive indices. The three-band model [34] describes the origins of the refractive indices for single LC compounds but requires three fitting parameters for each LC compound. The original Cauchy's equation [35]

TABLE 5. Cauchy Constants for 10O.O3 and 10O.O6 Pure LC Compounds with Dispersion of 1 wt% ZnO Nanoparticles

T, °C	Model	A_e	B_e, μm^2	C_e, μm^4	R^2	A_o	B_o, μm^2	C_o, μm^4	R^2
10O.O3 pure									
135. 4	2	1.5603	0.0186		0.9796	1.4806	0.1149		0.9723
	3	1.4581	0.0467	–0.0036	0.9730	1.4290	0.0420	–0.0042	0.9825
132.8	2	15104	0.0186		0.9796	1.4778	0.1149		0.9723
	3	1.4622	0.0467	–0.0036	0.9703	1.4262	0.0420	–0.0042	0.9825
10O.O3 with 1 wt% ZnO NPs									
103.6	2	1.4821	0.01562		0.9918	1.4785	0.0101		0.9876
	3	1.5086	0.0294	–0.0019	0.9880	1.4497	0.2538	–0.0021	0.9915
103.0	2	1.5118	0.0156		0.9918	1.450	0.0101		0.9876
	3	1.4885	0.2948	–0.0019	0.9880	1.438	0.013	–0.0021	0.9873
10O.O6 pure									
105.4	2	1.5721	0.0102		0.9702	1.5338	0.0089		0.9722
	3	1.5832	0.0034	–0.0009	0.9436	1.5206	0.0131	–0.0005	0.9436
104.8	2	1.5749	0.0100		0.9702	1.5302	0.0089		0.9722
	3	1.5806	0.0034	–0.0009	0.9436	1.5232	0.014	–0.0005	0.9436
10O.O6 with 1 wt% ZnO NPs									
105.7	2	1.5257	0.0091		0.9656	1.4787	0.0064		0.9436
	3	1.4964	0.0262	–0.0023	0.9506	1.4419	0.0283	–0.0030	0.9456
105.1	2	1.5225	0.0091		0.9656	1.4787	0.0064		0.9436
	3	1.4936	0.0262	–0.0023	0.9505	1.4451	0.00283	–0.0030	0.9456

was intended for isotropic gases and liquids. It has been attempted to fit the wavelength-dependent refractive indices of some anisotropic liquid crystals [30]. The fitting results are reasonably good except that the physical origins of Cauchy's coefficients are not clear. The LC birefringence is below 0.12, and the three-coefficient Cauchy's equations can be reduced to two-coefficient ones [31].

Cauchy's equations can be applied to single compounds as well as mixtures, whereby once A, B, and C coefficients are determined, the refractive indices of LC at any wavelength can be extrapolated. However, there are three Cauchy coefficients involved for each refractive index. It is highly desirable to reduce the number of the fitting parameters. For a low birefringence, a LC compound in the off-resonance region (C_e/λ^4) term is relatively small. Therefore, one can reduce the fitting parameters to two, by ignoring the third term (λ^{-4}). Accordingly, Eqs. (13) and (17) can be reduced and represented as Eqs. (21) and (22). From the preceding equations, it is evident that there are two coefficients for each refractive index. With the help of Cauchy's coefficients, the refractive index of the material can be measured at any wavelength. The LC compounds of 10O.O6 and 10O.O3 along with 1 wt% of ZnO NPs are calculated from RI values of n_e and n_o to validate the Cauchy models, and the values are presented in Table 4. The units of Cauchy's constants B and C are μm^2 and μm^4, respectively. R^2 is called the regression or correlation coefficient. For 10O.O3 pure and LC ZnO nanocomposites, the three-coefficient model is more fit than the two-coefficient model and for 10O.O6 pure and LC ZnO nanocomposites, the two-coefficient model is more fit than the three-coefficient model.

Conclusions. In the present study, 10O.O*m* LC (m = 3, 6) compounds with uniform dispersion of 1 wt% ZnO NPs have been prepared. The size of ZnO nanoparticles is calculated with XRD studies. The morphological information of ZnO nanoparticles has been obtained with SEM along with EDS data. The phase change temperatures obtained with the polarizing optical microscopy are found to be compatible with those obtained with DSC. The refractive indices n_e and n_o of 10O.O*m* and LC nanocomposites with 1 wt% dispersion of ZnO NPs at various wavelengths (460, 500, 570, and 635 nm) revealed that the separation between n_e and n_o is decreased in the stabilized nematic region. Further, the orientational order parameter of 10O.O*m* LC compounds is decreased due to the dispersion of 1 wt% ZnO NPs. Additionally, the nematic thermal ranges are increased and the smectic ranges are quenched. Due to the localized defects, the re-orientation takes place between LC and NPs, which makes the reorientation of LCs harder and causes the disorder. Thereby, the orientational order parameter is decreased and the anisotropic nature of 10O.O*m* liquid crystalline compounds is decreased, which, in turn, enhances the electro-optical properties of LC devices.

REFERENCES

1. H. K. Bisoyi, S. Kumar, *Chem. Soc. Rev*., **40**, 306–319 (2011).
2. G. W. Gray, In: *Handbook of Liquid Crystals*, Eds. D. Demus, J. Goodby, G. W. Gray, H. W. Spiess, V. Vill, Vol. 1, Wiley-VCH, Weinheim, 1–16 (1998).
3. S. Gauza, C. H. Wen, S. T. Wu, N. Janarthanan, C. S. Hsu, *J. Appl. Phys*., **43**, 7634–7638 (2004).
4. S. T. Wu, Q. T. Zhang, S. Marder, *Jpn. J. Appl. Phys*., **37**, L1254–L1256 (1998).
5. S. K. Prasad, M. V. Kumar, C. V. Yelamaggad, *Carbon*, **59**, 512–517 (2013).
6. J. Branch, R. Thompson, J. W. Taylor, L. Salamanca-Riba, L. J. Martínez-Miranda, *J. Appl. Phys*., **115**, 164313 (2014).
7. L. Marino, S. Marino, D. Wang, E. Bruno, N. Scaramuzza, *Soft Matter*, **10**, 3842–3849 (2014).
8. A. Chandran, J. Prakash, K. K. Naik, A. K. Srivastava, R. Dąbrowski, M. Czerwiński, A. J. Biradar, *J. Mater. Chem*., **C2**, 1844–1853 (2014).
9. P. Goel, M. Arora, A.M. Biradar, *J. Appl. Phys.*, **115**, 124905 (2014).
10. L. Wang, W. L. He, X. Xiao, M. Wang, P. Y. Yang, Z. J. Zhou, H. Yang, H. F. Yu, Y. F. Lu, *Mater. Chem.*, **22**, 19629–19633(2012).
11. X. W. Zhang, D. Luo, Y. Li, M. Zhao, B. Han, M. T. Zhao, H. T. Dai, *Liq. Cryst.*, **42**, 1257–1263 (2015).
12. U. Manzoor, M. Islam, L. Tabassam, S. U. Rahman, *Phys. E*, **41**, 1669–1672 (2015).
13. J. C. Nie, J. Y. Yang, Y. Piao, H. Li, Y. Sun, Q. M. Xue, C. M. Xiong, R. F. Dou, Q. Y. Tu, *Appl. Phys. Lett*., **93**, 173104 (2008).
14. A. V. Kabashin, A. Trudeau, W. Marine, *Appl. Phys. Lett*., **91**, 201101 (2007).
15. S. D. Haranath, A. G. Sahai, B. K. Joshi Gupta, *Nanotech*., **20**, 42570 (2009).
16. X. D. Li, T. P. Chen, P. Liu, Y. Liu, K. C. Leong, *Opt. Express*, **21**, 14131–14138 (2013).
17. A. L. Schoenhalz, J. T. Arantes, A. Fazzio, G. M. Dalpian, *J. Phys. Chem. C*, **114**, 18293–18297 (2010).
18. P. Khushboo Sharma, P. Malik, K. K. Raina, *Liq. Cryst*., **44**, 1717–1726 (2017).

19. K. Pal, S. Thomas, M. L. N. M. Mohan, *J. Nanosci. Nanotech*., **17**, 2401–2412 (2017).
20. W. Lee, C.-Y. Wang, Y.-C. Shih, *Appl. Phys. Lett.*, **85**, 513–515 (2004).
21. W. T. Chen, P. S. Chen, C. Y. Chao, *Jpn. J. Appl. Phys.*, **48**, 015006 (2009).
22. N. Kapernaum, F. Giesselmann, *Phys. Rev. E*, **78**, 062701 (2008).
23. I. Haller, *Prog. Solid State Chem*., **10**, 103–118 (1975).
24. H. J. Kim, Y. G. Kang, H. G. Park, K. M. Lee, H. Y. Jung, D. S. Seo, *Liq. Cryst*., **38**, 871–875 (2011).
25. G. Pathaka, R. Katiyara, K. Agraharia, A. Srivastavaa, R. Dabrowskib, K. Garbatb, R. Manohara, *Opto-Electron. Rev*., **26**, 11–18 (2018).
26. H. Eskalen Özgan, O. Alver, S. Kerli, *Acta Phys. Polonica A*, **127**, 756–760 (2015).
27. L. J. Martínez-Miranda, K. M. Traister, I. Meléndez- Rodríguez, *Appl. Phys. Lett*., **97**, 223301 (2010).
28. P. V. Raja Shekar, D. Madhavi Latha, V. G. K. M. Pisipati, *Opt. Mater*., **64**, 564–568 (2017).
29. S.-T. Wu, *Phys. Rev. A*, **33**, No. 2, 1270–1274 (1986).
30. H. Mada, S. Kobayashi, *Mol. Cryst. Liq. Cryst*., **33**, No. 1-2, 47–53 (1976).
31. J. Li, S.-T. Wu, *J. Appl. Phys*., **96**, No. 1, 170–174 (2004).
32. L. M. Blinov, *Electro-Optical and Magneto-Optical Properties of Liquid Crystals*, Wiley, New York (1983).
33. S. T. Wu, *J. Appl. Phys*., **69**, 2080–2087 (1991).
34. S. T. Wu, C. S. Wu, M. Warenghem, M. Ismaili, *Opt. Eng*., **32**, 1775–1780 (1993).
35. E. M. Averyanov, *J. Opt. Technol*., **64**, 417 (1997).